

Superscaling in Charged Current Neutrino Quasielastic Scattering in the Relativistic Impulse Approximation

J. A. Caballero,¹ J. E. Amaro,² M. B. Barbaro,³ T. W. Donnelly,⁴ C. Maieron,⁵ and J. M. Udias⁶

¹*Departamento de Física Atómica, Molecular y Nuclear, Universidad de Sevilla, 41080 Sevilla, Spain*

²*Departamento de Física Moderna, Universidad de Granada, 18071 Granada, Spain*

³*Dipartimento di Fisica Teorica, Università di Torino and INFN, Sezione di Torino, Via P. Giuria 1, 10125 Torino, Italy*

⁴*Center for Theoretical Physics, Laboratory for Nuclear Science and Department of Physics, Massachusetts Institute of Technology, Cambridge, Massachusetts 02139, USA*

⁵*INFN, Sezione di Catania, Via Santa Sofia 64, 95123 Catania, Italy*

⁶*Departamento de Física Atómica, Molecular y Nuclear, Universidad Complutense de Madrid, 28040 Madrid, Spain*

(Received 13 April 2005; published 15 December 2005)

Superscaling of the quasielastic cross section in charged-current neutrino-nucleus reactions at energies of a few GeV is investigated within the framework of the relativistic impulse approximation. Several approaches are used to describe final-state interactions and comparisons are made with the plane-wave approximation. Superscaling is very successful in all cases. The scaling function obtained using a relativistic mean field for the final states shows an asymmetric shape with a long tail extending towards positive values of the scaling variable, in excellent agreement with the behavior presented by the experimental scaling function.

DOI: [10.1103/PhysRevLett.95.252502](https://doi.org/10.1103/PhysRevLett.95.252502)

PACS numbers: 25.30.Pt, 13.15.+g, 24.10.Jv

In the context of inclusive quasielastic (QE) electron scattering at intermediate to high energies, the concepts of scaling [1] and superscaling [2] have been explored in previous work [3,4], where an exhaustive analysis of the (e, e') world data demonstrated the quality of the scaling behavior. Scaling of the first kind (no dependence on the momentum transfer) is reasonably well respected at excitation energies below the QE peak, whereas scaling of the second kind (no dependence on the nuclear species) is excellent in the same region. The simultaneous occurrence of both kinds of scaling is called superscaling. At energies above the QE peak both scaling of the first and, to a lesser extent, of the second kind are shown to be violated because of important contributions introduced by effects beyond the impulse approximation, namely, inelastic scattering [5] together with correlations and meson exchange currents in both the $1p-1h$ and $2p-2h$ sectors [6,7].

The scaling analysis of (e, e') data has recently been extended through the QE peak into the Δ region [8]. Of relevance to the present work we note that the high-energy inclusive electron scattering cross section is well represented up to the Δ peak using the scaling ideas, importantly, with an *asymmetric* QE scaling function. In that study the scaling approach was also used to predict nuclear (ν, μ) cross sections, based on the assumption of a universal scaling function, valid for both electron and neutrino scattering at corresponding kinematics.

In this Letter we investigate the QE scaling properties of charged-current (CC) neutrino-nucleus scattering within the context of the relativistic impulse approximation (RIA). After verifying that various RIA models do superscale, we compare the associated scaling functions with the (e, e') phenomenological one referred to above. This allows a check on the consistency of the universality as-

sumption and on the capabilities of different models to yield the required properties of the experimental scaling function, specifically, its asymmetric form.

Here we follow the general procedure of scaling and superscaling studies, namely, we first construct inclusive cross sections within a model and then obtain scaling functions by dividing them by the relevant single-nucleon cross sections weighted by the corresponding proton and neutron numbers [3,4,9]. The scaling function is plotted against the scaling variable $\psi(q, \omega)$, with q and ω the momentum and energy transferred in the process, and its scaling properties analyzed.

Within the RIA framework CC neutrino-nucleus QE scattering is described by assuming that at the $\nu\text{-}\mu$ vertex one vector boson is exchanged with the nucleus, interacting with only one nucleon, which is then emitted while the remaining ($A-1$) nucleons in the target remain as spectators. The nuclear current operator is thus taken to be the sum of single-nucleon currents, for which we employ the usual relativistic free nucleon expressions [8,10]. The RIA approach has been extensively and successfully applied in investigations of exclusive electron scattering reactions [11]. Further details on the model have been presented in Refs. [10,12,13].

We describe the bound nucleon states as self-consistent Dirac-Hartree solutions, derived within a relativistic mean field (RMF) approach using a Lagrangian containing σ , ω , and ρ mesons [14]. For the description of the outgoing nucleon states we consider several different approaches. In one we use plane-wave spinors [thus no final-state interactions (FSI)], corresponding to the relativistic plane-wave impulse approximation (RPWIA). However, comparisons with data require a more realistic description of the final nucleon state, which should include the effects due to FSI.

This is accomplished by using solutions of a Dirac equation containing relativistic potentials. This constitutes the relativistic distorted-wave impulse approximation.

The use of complex relativistic optical potentials fitted to elastic proton scattering data has proven to be successful in describing *exclusive* ($e, e'p$) scattering reactions [11]. The absorption produced by the imaginary term represents the loss of flux into inelastic channels. For *inclusive* processes such as (e, e') and (ν, μ), where a selection of the exclusive single-nucleon knockout channel cannot be made, the contribution from these inelastic channels should be retained. Ignoring them would lead to an underestimation of the inclusive cross section [13]. A simple way of obtaining the right inclusive strength within the RIA is to use purely real potentials. We consider two choices for the real part. The first uses the phenomenological relativistic optical potential from the energy-dependent, A -independent parametrizations (EDAIC, EDAIO, EDAICa) derived by Clark *et al.* [15], but with their imaginary parts set to zero. The second approach employs distorted waves obtained with the same relativistic mean field used to describe the initial bound nucleon states. We refer to these two FSI descriptions as real relativistic optical potential (rROP) and RMF, respectively. Dispersion relation and Green function techniques have been used to rigorously derive the potentials for inclusive scattering (see Refs. [16–18]) leading to results which are within a few percent of those obtained in the IA with either the rROP [18] or the mean field [16]. Note that the RMF model (1) is known to work quite well for inclusive QE (e, e') scattering (which is verified here; see below) and (2) is constructed in a way that fulfills the dispersion relation [16] and maintains the continuity equation.

Our results for CC neutrino-nucleus QE scattering are presented in Fig. 1, where we show the differential cross section ($d\sigma/dE_\mu d\Omega_\mu$) as a function of the outgoing muon kinetic energy for ^{12}C and ^{16}O . For reference we also include the results obtained within the relativistic Fermi

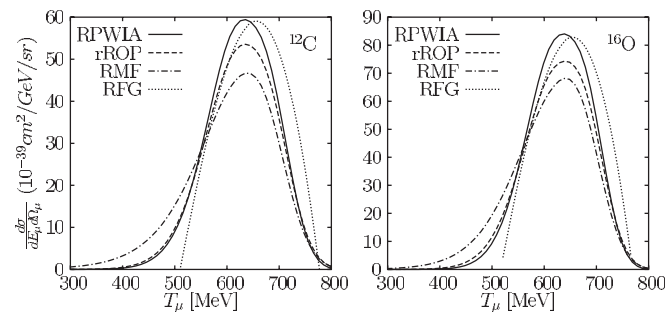


FIG. 1. Quasielastic differential cross section $d\sigma/dE_\mu d\Omega_\mu$ versus the muon kinetic energy T_μ for the reaction (ν_μ, μ^-) on ^{12}C (left) and ^{16}O (right). The incident neutrino energy is $\varepsilon_\nu = 1$ GeV and the muon scattering angle is $\theta_\mu = 45^\circ$. In each panel we present results for RPWIA (solid line), rROP (dashed line) and RMF (dot-dashed line). The cross section for the RFG model is also presented for reference (dotted line).

gas (RFG) (dotted) with Fermi momenta $k_F = 228$ MeV/ c for ^{12}C [4] and $k_F = 216$ MeV/ c for ^{16}O [19]. The RFG curves contain a phenomenological energy shift [4] yielding RFG cross sections which are very similar to the RPWIA results.

The mean field dynamics in the initial and final nuclear states lead to cross sections having tails that extend both below and above the kinematical region where the RFG is defined. With FSI included we observe a reduction of the cross section, particularly in the case of the RMF potential where it is seen to be about 20% for both nuclei in the region close to the maximum. Notice also a slight displacement in the maximum of the cross section in the cases of the two RIA-FSI models. However, the most striking feature is the long tail displayed by the RMF cross section for small muon kinetic energies. This corresponds to transferred energies above the QE peak, i.e., positive values of the scaling variable. These FSI effects lead to a clear asymmetry in the RMF cross section, in contrast to the RPWIA and rROP results. The discrepancy between the two FSI approaches is linked to the different behaviors of the two potentials: for high nucleon kinetic energies (small muon energies) the scalar and vector energy-dependent potentials of the rROP model are significantly reduced with respect to the RMF [11]. The latter approach has strong scalar and vector potentials that are delicately balanced and that shift the strength towards higher energies. This explains why the rROP cross section is closer to the RPWIA case, and moreover, why the main difference between the two models is observed in the region of lower muon energies. Note that the asymmetric broadening of the RMF cross section is similar to that observed in nonrelativistic models of the FSI, described by some as medium modifications of the p - h propagator [19].

Let us now study the superscaling properties. We present results for the scaling function $f(\psi')$, which is obtained by dividing the calculated differential cross section of Fig. 1 by the single-nucleon cross section as given in Eqs. (45,52,86–94) of Ref. [8]. This function is plotted against the shifted QE scaling variable ψ' defined as

$$\psi' \equiv \frac{1}{\sqrt{\xi_F}} \frac{\lambda' - \tau'}{\sqrt{(1 + \lambda')\tau' + \kappa\sqrt{\tau'(1 + \tau')}}}, \quad (1)$$

where $\lambda' \equiv (\omega - E_{\text{shift}})/2m_N$, $\kappa \equiv q/2m_N$, $\tau' \equiv \kappa^2 - \lambda'^2$, and $\xi_F \equiv \sqrt{1 + (k_F/m_N)^2} - 1$. The energy shift E_{shift} has been taken from Ref. [4]. Results correspond to fixed scattering muon angle $\theta_\mu = 45^\circ$, although similar scaling functions are obtained with other values.

Scaling of the first kind is explored in Fig. 2, where we present $f(\psi')$ for ^{12}C at three different values of the incident energy. Each panel in the figure corresponds to a different description of the FSI. As one can see, the scaling function for the RPWIA and rROP models shows a very mild dependence on the momentum transfer in both positive and negative ψ' regions. In the case of the RMF, a

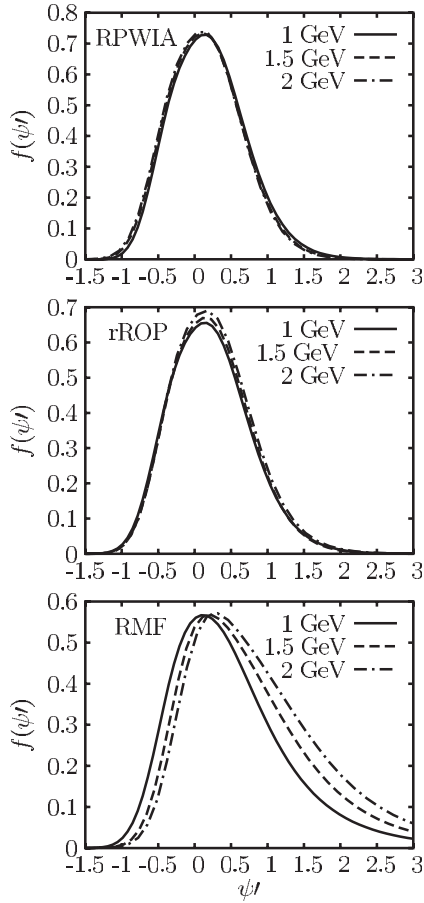


FIG. 2. Scaling function for three values of the incident neutrino energy ε_ν . Results correspond to ^{12}C and $\theta_\mu = 45^\circ$. Top, middle, and bottom panels refer to RPWIA, rROP, and RMF models (see text for details).

slight shift occurs in the so-called “scaling region” $\psi' < 0$, whereas for ψ' positive the model breaks scaling at roughly the 30% level in the energy region explored here. This is not in conflict with the experimental (e, e') data that indeed leave room for some breaking of first-kind scaling in this region, due partly to Δ production and partly to other contributions, such as meson exchange currents and their associated correlations in the $2p$ - $2h$ sector [7]. It is striking that the RMF model, in spite of being based on the impulse approximation, leads to the same kind of behavior which is apparently not reproduced by uncorrelated models in the impulse approximation. Importantly, the RMF scaling function exhibits a significant asymmetry, being larger for positive ψ' , which persists for all neutrino energies (actually increasing with ε_ν).

Scaling of the second kind is studied in Fig. 3, where the scaling function evaluated for three nuclei is presented using the three models. The values of the Fermi momentum used range from $k_F = 216$ MeV/ c for ^{16}O to $k_F = 241$ MeV/ c for ^{40}Ca [4]. The initial bound states have been obtained using the parameters of the set NLSH [20]. Results with other parametrizations are similar and

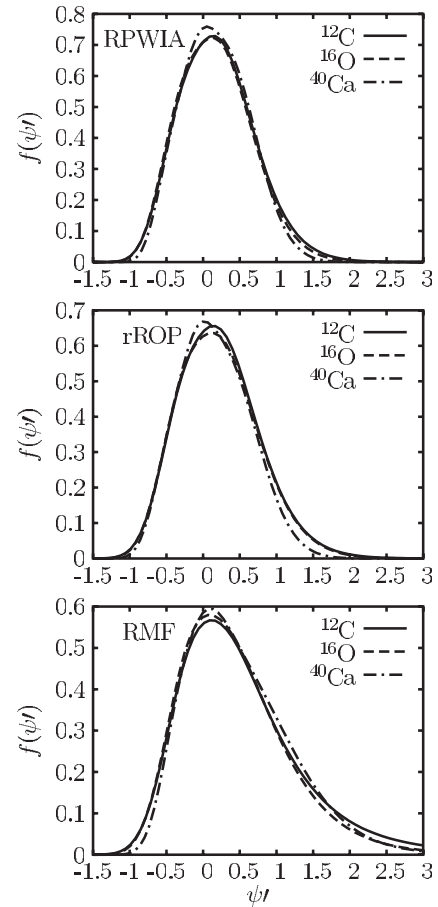


FIG. 3. Scaling function for three nuclei: ^{12}C , ^{16}O and ^{40}Ca . Results correspond to $\varepsilon_\nu = 1$ GeV and $\theta_\mu = 45^\circ$. Top, middle, and bottom panels as in previous figure.

do not change the general conclusions. As observed, the differences introduced by changing nucleus are small. We may conclude that within the present model scaling of the second kind is very successful. Indeed, this is just what is seen experimentally, at least for $\psi' < 0$ where scaling of the second kind is excellent [2,3].

Finally, in Fig. 4 we compare the model superscaling functions with the averaged QE phenomenological function obtained from the analysis of (e, e') data [2,8,21].

First we observe the symmetric character of the RPWIA and rROP results, which clearly differ from the experimental function. On the contrary, the RMF curve displays a pronounced tail that extends toward positive values of ψ' , following closely the asymmetric behavior of the data and yielding excellent agreement with the phenomenological scaling function. In the light of the analysis in Ref. [8] this immediately implies that the RMF approach yields excellent agreement with the experimental (e, e') inclusive cross section. The asymmetric shape of the RMF result constitutes a basic difference not only from the other two models explored in this work, but also from other modeling presented in the literature, such as those in Ref. [22], where the long tail in the superscaling function is absent. Indeed,

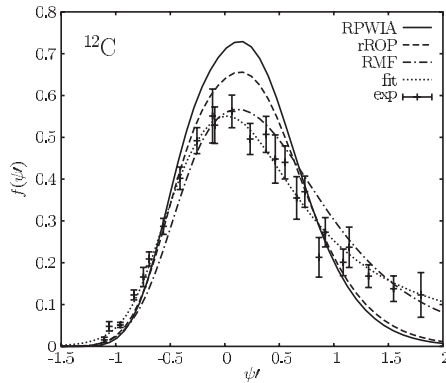


FIG. 4. Scaling function evaluated within the RPWIA (solid line), rROP (dashed line) and RMF (dot-dashed line) approaches compared with the averaged experimental function together with a phenomenological parametrization of the data (dotted line).

the coherent density fluctuation model for correlation effects presented in Ref. [22] is manifestly symmetrical around the QE peak. It should be remarked that all of the curves in Fig. 4 essentially satisfy the Coulomb sum rule; i.e., they integrate to unity.

The results in Fig. 4 demonstrate that the RMF model is successful at incorporating important dynamical effects missed by the other models [23]. Only in the RMF case is the required asymmetric form of the scaling function obtained. It should be stressed that the main factors responsible for the asymmetry in the calculated scaling function are not only relativity (present in all models considered here), but the particular description of the final continuum nucleon states. The asymmetry observed in the data has usually been ascribed to the role played by ingredients beyond the mean field, such as short-range correlations and two-body currents [7]. We show here that it can be explained within the RIA framework resorting only to one-body excitations, provided strong relativistic potentials are included in the model. It would be interesting to see how a more elaborated formalism that includes multi-nucleon excitations as in Ref. [17] compares with super-scaling data.

In summary, we have shown that superscaling is fulfilled to high accuracy within the present relativistic impulse approximation in the QE region, and that this holds for the three different descriptions of FSI considered here. The asymmetric shape and the long tail at positive ψ' values observed in the experimental scaling function is reproduced only by the RMF model. This result reinforces our confidence in the adequacy of descriptions of FSI effects for inclusive (e, e') and (ν, μ) reactions when based on the RMF approach.

This work was partially supported by DGI (Spain): BFM2002-03315, BFM2002-03218, FPA2002-04181-C04-04, BFM2003-041-C02-01, by the Junta de Andalucía, and by the INFN-CICYT collaboration agreement No. 04-17. It was also supported in part (T. W. D.) by U.S.

Department of Energy under Cooperative Agreement No. DE-FC02-94ER40818.

- [1] G. B. West, Phys. Rep. **18**, 263 (1975); D. B. Day, J. S. McCarthy, T. W. Donnelly, and I. Sick, Annu. Rev. Nucl. Part. Sci. **40**, 357 (1990).
- [2] T. W. Donnelly and I. Sick, Phys. Rev. Lett. **82**, 3212 (1999).
- [3] T. W. Donnelly and I. Sick, Phys. Rev. C **60**, 065502 (1999).
- [4] C. Maieron, T. W. Donnelly, and I. Sick, Phys. Rev. C **65**, 025502 (2002).
- [5] L. Alvarez-Ruso, M. B. Barbaro, T. W. Donnelly, and A. Molinari, Nucl. Phys. **A724**, 157 (2003); M. B. Barbaro, J. A. Caballero, T. W. Donnelly, and C. Maieron, Phys. Rev. C **69**, 035502 (2004).
- [6] J. E. Amaro, M. B. Barbaro, J. A. Caballero, T. W. Donnelly, and A. Molinari, Nucl. Phys. **A697**, 388 (2002); **A723**, 181 (2003); Phys. Rep. **368**, 317 (2002).
- [7] A. De Pace, M. Nardi, W. M. Alberico, T. W. Donnelly, and A. Molinari, Nucl. Phys. **A741**, 249 (2004); **A726**, 303 (2003).
- [8] J. E. Amaro *et al.*, Phys. Rev. C **71**, 015501 (2005).
- [9] M. B. Barbaro, R. Cenni, A. De Pace, T. W. Donnelly, and A. Molinari, Nucl. Phys. **A643**, 137 (1998).
- [10] W. M. Alberico *et al.*, Nucl. Phys. **A623**, 471 (1997).
- [11] J. M. Udías *et al.*, Phys. Rev. C **48**, 2731 (1993); **51**, 3246 (1995); **64**, 024614 (2001).
- [12] W. M. Alberico *et al.*, Phys. Lett. B **438**, 9 (1998); Nucl. Phys. **A651**, 277 (1999).
- [13] C. Maieron, M. C. Martínez, J. A. Caballero, and J. M. Udías, Phys. Rev. C **68**, 048501 (2003); Y. Jin, D. S. Onley, and L. E. Wright, Phys. Rev. C **45**, 1333 (1992); K. S. Kim and L. E. Wright, Phys. Rev. C **68**, 027601 (2003).
- [14] C. J. Horowitz and B. D. Serot, Nucl. Phys. **A368**, 503 (1981); Phys. Lett. B **86**, 146 (1979); B. D. Serot and J. D. Walecka, Adv. Nucl. Phys. **16**, 1 (1986).
- [15] E. D. Cooper, S. Hama, B. C. Clark, and R. L. Mercer, Phys. Rev. C **47**, 297 (1993).
- [16] Y. Horikawa, F. Lenz, and N. C. Mukhopadhyay, Phys. Rev. C **22**, 1680 (1980).
- [17] C. R. Chinn, A. Picklesimer, and J. W. Van Orden, Phys. Rev. C **40**, 790 (1989).
- [18] A. Meucci, F. Capuzzi, C. Giusti, and F. Pacati, Phys. Rev. C **67**, 054601 (2003).
- [19] G. Co', C. Bleve, I. De Mitri, and D. Martello, Nucl. Phys. B, Proc. Suppl. **112**, 210 (2002); C. Bleve *et al.*, Astropart. Phys. **16**, 145 (2001); J. Nieves, J. E. Amaro, and M. Valverde, Phys. Rev. C **70**, 055503 (2004).
- [20] M. M. Sharma, M. A. Nagarajan, and P. Ring, Phys. Lett. B **312**, 377 (1993).
- [21] J. Jourdan, Nucl. Phys. **A603**, 117 (1996).
- [22] J. E. Amaro, M. B. Barbaro, J. A. Caballero, T. W. Donnelly, and C. Maieron, Phys. Rev. C **71**, 015501 (2005); A. N. Antonov *et al.*, Phys. Rev. C **69**, 044321 (2004); **71**, 014317 (2005).
- [23] J. M. Udías, P. Sarriguren, E. Moya de Guerra, and J. A. Caballero, Phys. Rev. C **53**, R1488 (1996).